

Article

# Thermal Comfort Improvement Strategies for Outdoor Spaces in Traditional Villages Based on ENVI-Met: Shimengao Village in Chizhou City

Tieqiao Xiao <sup>1,2</sup>, Lanlan Sheng <sup>1</sup>, Shaojie Zhang <sup>1,\*</sup>, Licheng Zheng <sup>1</sup> and Taotao Shui <sup>3</sup>

<sup>1</sup> Anhui Academy of Territory Spatial Planning & Ecology, Hefei 230601, China; xtg020032@ahjzu.edu.cn (T.X.); sll0801@stu.ahjzu.edu.cn (L.S.); 19156453454@163.com (L.Z.)

<sup>2</sup> School of Architecture & Urban Planning, Anhui Jianzhu University, Hefei 230601, China

<sup>3</sup> School of Environment and Energy Engineering, Anhui Jianzhu University, Hefei 230601, China; shuitaotao@ahjzu.edu.cn

\* Correspondence: shaojiezhong@ahjzu.edu.cn

**Abstract:** The thermal comfort of outdoor spaces in traditional villages must be improved because high building density combined with complex and narrow spaces leads to a poor thermal environment. In traditional villages, outdoor spaces are the most frequently used places by local residents and tourists. In this study, the Shimengao Village in Tangxi Town, Chizhou City, a typical mountainous area in the southern Anhui Province, was selected as the research object, and Depthmap software was used to identify the most frequently used outdoor spaces. The spatial layout and three different outdoor spaces of the traditional village were measured and validated using ENVI-met software. In addition, the distribution of thermal comfort in the core area of the village and influencing factors were analyzed. Our results demonstrated that during summer, PET reached its highest value at 15:00, exhibiting a poor thermal environment in the core area of traditional village integration. From 15:00 to 21:00, PET values declined, resulting in improved thermal comfort levels. Open spaces had better thermal comfort ratings throughout the day. The thermal comfort distribution of three different types of outdoor space in traditional villages was also analyzed. The courtyard space had the worst thermal comfort, followed by the street space, whereas the square space had the best thermal comfort environment. This was correlated with the spatial layout of traditional villages, external facilities of buildings, microlandscapes (plants, water availability, etc.), and outdoor ground materials. Hence, we propose that optimizing the overall spatial layout of a traditional village, increasing the external facilities of buildings, creating “micro landscapes,” and optimizing the materials of outdoor spaces are important for improving the thermal comfort of the outdoor spaces of traditional villages.

**Keywords:** ENVI-met; improvement strategy; physiological equivalent temperature; traditional village; spatial layout; spatial syntax



**Citation:** Xiao, T.; Sheng, L.; Zhang, S.; Zheng, L.; Shui, T. Thermal Comfort Improvement Strategies for Outdoor Spaces in Traditional Villages Based on ENVI-Met: Shimengao Village in Chizhou City. *Sustainability* **2023**, *15*, 11785. <https://doi.org/10.3390/su151511785>

Academic Editors: Andrea De Montis, Antonio Ledda and Vittorio Serra

Received: 2 June 2023

Revised: 12 July 2023

Accepted: 28 July 2023

Published: 31 July 2023



**Copyright:** © 2023 by the authors. Licensee MDPI, Basel, Switzerland. This article is an open access article distributed under the terms and conditions of the Creative Commons Attribution (CC BY) license (<https://creativecommons.org/licenses/by/4.0/>).

## 1. Introduction

With the continuous improvement in science, technology, and their living standards, people have increased their requirements for outdoor-space habitats in traditional villages [1]. The outdoor spaces of traditional villages are places to which local residents and tourists frequently travel. At the same time, the population of traditional villages is increasingly aging, with the elderly people often choosing outdoor cooling in the summer, especially under the shade of trees and buildings, because of economic and physical reasons. As such, improving their thermal comfort is conducive to a better life for local residents and the development of the local tourism industry. Thus, it is of practical significance to propose targeted strategies for improving thermal comfort in traditional villages.

Thermal comfort is the degree of subjective satisfaction with the external environment, as perceived by people. External environmental parameters include temperature, relative

humidity, and airflow rate. In this study, the focus was placed on thermal comfort in different outdoor spaces. In the past two decades, many scholars have examined strategies to improve thermal comfort, primarily through the arrangement of plants [2,3], selection of tree species [3,4], selection of materials for different reflective outdoor spaces [5–7], and creation of water bodies [8,9]. In 2016, Morakinyo et al. used physiological equivalent temperature (PET) to characterize the thermal comfort of canyons by studying the influence of different planting patterns, arrangements, and orientation on the thermal comfort of street canyons and found that the PET value of double-row and east-oriented planting was higher than that of central planting [10]. In 2023, Deng et al. studied *Ficus altissima* trees, a common subtropical tree species, and found that different canopy directions had certain effects on temperature, humidity, and wind speed. In particular, the study found that a dense canopy reduced the air temperature, especially under shade, and improved thermal comfort [11]. In 2023, Thomas et al. used ENVI-met software to study the impact of different reflectance cushions on the ambient air temperature of the campus and found that the implementation of green walls provided a certain shading effect and reduced the ambient air temperature of the campus to the maximum; a reduction of 1.3–1.6 °C in winter and 0.4–0.5 °C in summer [12]. In 2022, Cheng et al. studied the relationship between building density, water body rate, and thermal comfort in a quantitative way, and identified a negative correlation between building density and thermal comfort. More specifically, they showed that the presence of a water body reduced the surrounding air temperature. During summer, the cooling effect of the water body in the afternoon was stronger than that in the morning, reaching its maximum effect between 12:00 and 15:00 [8].

Based on these results, scholars have conducted studies to strategically increase thermal comfort in the countryside. Accordingly, we used these generalizable results as the basis for this study. However, most of these studies have mainly focused on the influence of a single factor from the study area on the microclimate of outdoor spaces while ignoring the interrelationship between multiple factors and the influence of different factors in combination with the microclimate [13]. In addition, most studies were modeled on general rural areas, whereas fewer studies have modeled traditional villages with complex spatial elements and irregular spatial composition [14]. Finally, most researchers have investigated the spatial morphology, wind speed and direction, and green-space rate, which are large-scale planning-control indexes and do not reflect the real nature and complexity of many study areas [15].

The present study used the Shimengao Village located in Tangxi Town, Chizhou City, China as the research object. We comprehensively considered the influence of various factors on the thermal comfort of villages, divided the outdoor space of traditional villages into three types, and simulated the thermal comfort distribution of typical outdoor spaces in the core area and three types of outdoor spaces of traditional villages during summer using ENVI-met measured data. Taking PET as the evaluation index of thermal comfort, we analyzed the factors affecting the thermal comfort of outdoor spaces. This study aimed to propose optimization strategies for improving the thermal comfort of outdoor spaces considering local characteristics. Some of these strategies include optimizing the overall spatial layout of traditional villages, increasing the external facilities of buildings, creating “micro-landscapes”, and changing the materials of outdoor spaces. The main aim was to propose an optimization strategy for improving the thermal comfort of outdoor spaces and provide a reference for the improvement of the habitats of traditional villages in typical mountainous areas.

The main objectives of this study were as follows: (1) to extract the integrated core area of the traditional villages in Shimen by using space syntax theory and to select three different types of outdoor spaces for measurement, (2) to use ENVI-met for simulating the integration core area and three different outdoor-space forms in traditional villages (square, street, and courtyard spaces), (3) to analyze the spatial and temporal distribution of the thermal comfort of these three types of outdoor spaces with traditional village

characteristics during the summer, and (4) to propose an outdoor-space optimization strategy for traditional villages based on improving thermal comfort.

## 2. Study Object

### 2.1. Site Overview

The Shimengao Village is located in Shimen Village, Tangxi Town, Chizhou City, Anhui Province (117°37' E, 30°21' N) in China, and is a typical traditional mountainous village. It belongs to the Cfa climate zone, which is consistent with the typical climate characteristics of regions with hot summers and cold winters [16]. The four seasons are characterized by “large differences in the Ta, a humid summer phase, significant seasonal wind speed changes, less sunlight and more annual precipitation”. The average annual Ta in Chizhou is 17.6 °C, with the average precipitation being 1294.7 mm. The dominant wind direction during summer is southwards, with the average wind speed being 1.52 m/s. The Shimengao Village covers an area of 4380 acres, with a building density of 18.4%. The village has an aging and declining population of 1323 residents that is divided into 12 groups. The buildings are low, consisting mainly of one or two stories (Table 1).

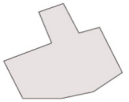



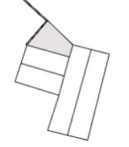
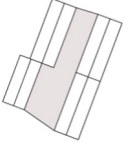
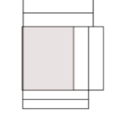
**Table 1.** Site overview.

Location	Chizhou (117°37' E, 30°21' N)
Population	1323
Building density	18.4%
Wind direction	S
Average wind speed	1.52 m/s
Average annual Ta	17.6 °C
Average precipitation	1294.7 mm
Average building height	1–2

Traditional villages have relatively stable spatial morphological characteristics, contain order and law, and their outdoor space reflects the local culture and its characteristics [17]. In this study, the spatial components of the integration core area were extracted, and outdoor spaces with traditional village culture and local characteristics were identified. The basic graphic language suitable for traditional villages in southern Anhui was determined via the decomposition and combination of “characters”, and “words” in different outdoor spaces. They are constructed in a certain order, and each element has its own specific spatial meaning. In this study, the spatial components of the integration core area were extracted and outdoor spaces with a traditional village culture and local characteristics were identified. The basic graphic language suitable for traditional villages in southern Anhui was determined via the decomposition and combination of “characters,” “words”, and “phrases” in different outdoor spaces. They are constructed in a certain order and each element has its own specific spatial meaning [18]. “Characters” primarily refers to the schema composed of a single element and “word” is a composite spatial schema formed by the combination of “characters” [19]. An investigation of the integration core space revealed that the “characters” schema primarily includes square space components, central surface water systems, linear water systems, courtyard-type space components, building setback square space components, and street-type space components. Three types of outdoor spaces (square, alley, and courtyard) were obtained from traditional village characteristics by arranging and combining the “characters” schema (Table 2).

This study primarily investigated the outdoor space environment of Shimen Gao Village, Tangxi Town, Guichi District, and Chizhou City and focused on the distribution of thermal comfort in different outdoor spaces. Due to computer performance limitations and the calculation rate of the simulation software, it was not possible to model the entire traditional village; therefore, three types of outdoor spaces of traditional villages in the core of the integrated and typical mountainous areas of southern Anhui were selected for the study: Kui Xing Square (square space), Old Street Lane (street space), and courtyard space.

**Table 2.** Three kinds of spatial recognition.

Location	Space Type	Characters	Graphical Language
Sample point 1	Plaza space	Square space components	
		linear water system	
		central surface water system	
Sample point 2	street space	linear water system	
		building setback square space components	
		alley-type space components	
Sample point 3	Courtyard space	courtyard-type space components	

## 2.2. Data Collection

A handheld anemometer was used for measuring wind speed. Measurements were taken on 8 July 2021, during a 12 h period between 7:00 and 19:00 under clear weather conditions. The equipment was adjusted to reduce errors before taking the measurements. Three different types of outdoor spaces were chosen as sample points: plaza, street, and courtyard spaces. Sample point 1 was located in Kui Xing Square, where the outdoor ground material was a mixture of cement and slate. Sample point 2 was located at Old Street Lane, where the outdoor ground material was granite. Sample point 3 was located at the intersection of Pepper House Lane (courtyard space), where the outdoor ground material was slate (Figure 1).

**Figure 1.** Sample points for measurements in the core area of integration.

The plaza space (sample point 1), in which local residents and visitors interact and relax for long periods, is located in the northcentral part of the village. The Gao Ancestral Hall is located on the north side, whereas the Fitness Square is on the west side of the square. A number of residential buildings on the east and south sides also have commercial functions. Of note, the outdoor ground material varies from north to south. Most structures on the southern and northern sides mostly consist of concrete and granite material, respectively. The center of the pond is surrounded by small trees. As the square is the most accessible outdoor space in the village, it is used for commercial and cultural activities.

The courtyard space (sample point 2), which is a semiopen space formed by two buildings, mainly serving residents, is located on the south side of the street space. Hence, it is the most frequently used place in the daily lives of residents. Courtyard spaces are often used by residents for activities such as sitting and drying clothes. The surrounding buildings have one or two stories and the courtyard lacks any vegetation. The two courtyard spaces examined in this study have irregular shapes with concrete outdoor flooring. Consequently, the thermal comfort level of the courtyard directly affects the habitat levels of local residents.

The street space (sample point 3) in the village is used by local residents and visitors for interaction and relaxation for long periods. With a total length of 186 m, the street is mostly surrounded by one-story Huizhou-style buildings. A nullah passes through the street with water plants growing around it and water flowing through it. The outdoor ground material consists of stone slabs. We conducted a thermal comfort analysis for a length of ~60 m in the old streets and alleys of the main block.

### 3. Research Methodology

#### 3.1. Spatial Syntactic Integration Analysis

Space syntax theory provides a variety of methods for the quantitative analysis of urban and rural spatial forms [20,21]. Axis is one of these methods, which represents the connections between spaces by reducing them to straight lines and by the connections between the lines [22]. The axis model is used to measure the degree of agglomeration or dispersion of space. A greater degree of agglomeration correlates with a higher utilization rate and more frequent use of space. The experimental area was considered in light of axis analysis theory in spatial syntax. In this study, the syntax model was used to calculate the integration degree of each axis using different colors to indicate the level of integration. Higher values indicate higher degrees of axis integration and the area surrounded by multiple axes of the highest integration degrees is called the core of the integration degree. A depth map was used to identify the core area of the outdoor spatial integration degree in Shimengao Village. A depth map is a measure of the degree of integration of a space with other spaces in the system, which can be perceived as the number of spatial steps needed to pass from one space to another. The higher the degree of integration, the stronger the association of space in the system with the system as a whole, the closer it is to other spaces, the smaller the number of spatial steps needed to pass between them, and the closer the connection [23].

BIO-met is a postprocessing tool that calculates human thermal comfort and a thermal comfort index based on simulated data. It can provide PET values and analyze the integration of the core area and the thermal comfort of different outdoor spaces. This study used the BIO-met plugin to model the core integration area and three different outdoor spaces and calculate thermal comfort values.

#### 3.2. ENVI-Met Modeling Setup

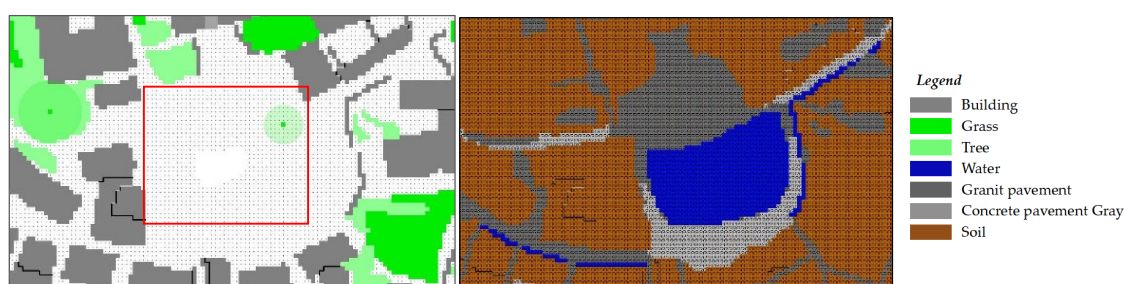
ENVI-met is the most commonly used numerical simulation research software to analyze the microclimate [24]. It is more adaptable to complex rural environments and contains scientifically accurate data. López-Cabeza et al., using the ENVI-met software to simulate the thermodynamic performance of courtyards during the design of buildings, found that the larger the size of the courtyard, the better the results of the simulations performed [25].



The relationship between the field measurements and the ENVI-met simulation results of thermal comfort in Port Said was demonstrated by Abd Elraouf et al. [26]. Liu used ENVI-met to simulate the microclimate based on the urban old residential area and established the microclimate model. The simulation result of the ENVI-met microclimate model agrees well with the measured data [27].

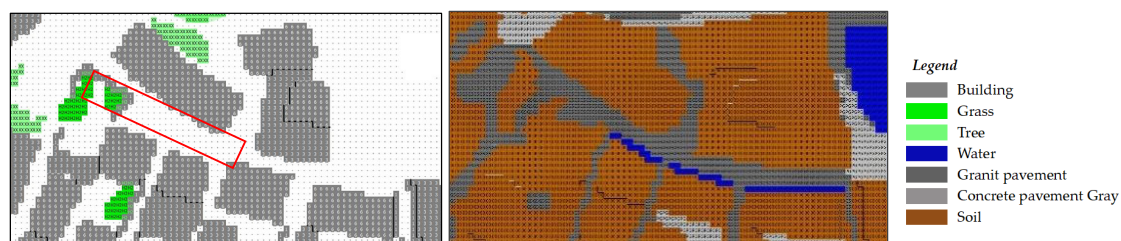
The buildings, outdoor spatial materials, waterbodies, and plants in the core model of traditional village integration were identified through field research. Residential buildings were found to consist mainly of one or two stories, consisting of wood and reinforced concrete. The resolution of different axes in the modeling software was  $1 \times 1 \times 0.5$  m, while the number of grids was  $230 \times 150 \times 40$  m. Floor and wall materials were available in the modeling tool and were modeled in space according to the actual location and nature of floor materials. Three kinds of outdoor spaces with traditional village characteristics were modeled: Kui Xing Square (square space), old streets and alleys (street space), and courtyard space.

The square space was located in the middle of the traditional village. It was composed of two parts: the northern part was mainly a rectangular square, whereas the southern part mainly consisted of a large water body. The surrounding buildings, similar to those in the rest of the village, were primarily one- or two-story buildings made of wood and reinforced concrete, with the outdoor-space material under the square being a mixture of cement and stone slabs. The square was surrounded by willow, balsam fir, and bitter tea trees, with the groundcover vegetation consisting mainly of spring and purple jasmine plants (Figure 2).



**Figure 2.** Sample point 1. Two-dimensional diagram and model underlay surface material.

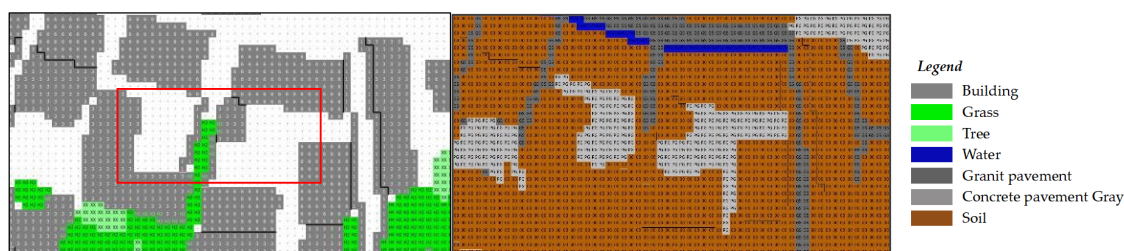
The street space was located on the west side of the square with a northwest–southeast alignment. It intersected with the square as a curved street, lined with mainly one- and two-story reinforced concrete buildings. The outdoor space of the street and alley was composed of granite. The surrounding area was dominated by willow, maple, and poplar tree species, as well as low shrubs, with the groundcover vegetation consisting of yingchun and deionberry plants (Figure 3).



**Figure 3.** Sample point 2. Two-dimensional diagram and model underlay surface material.

The courtyard space was located on the south side of the square and street; this space was U-shaped and enclosed by three buildings. The surrounding buildings were two-story houses made of wood and reinforced concrete, while the outdoor space of the courtyard consisted of stone slabs. The surrounding area mainly included maple, poplar,

and bittersweet trees, with the groundcover vegetation consisting mainly of spring begonia and purple jasmine plants (Figure 4).



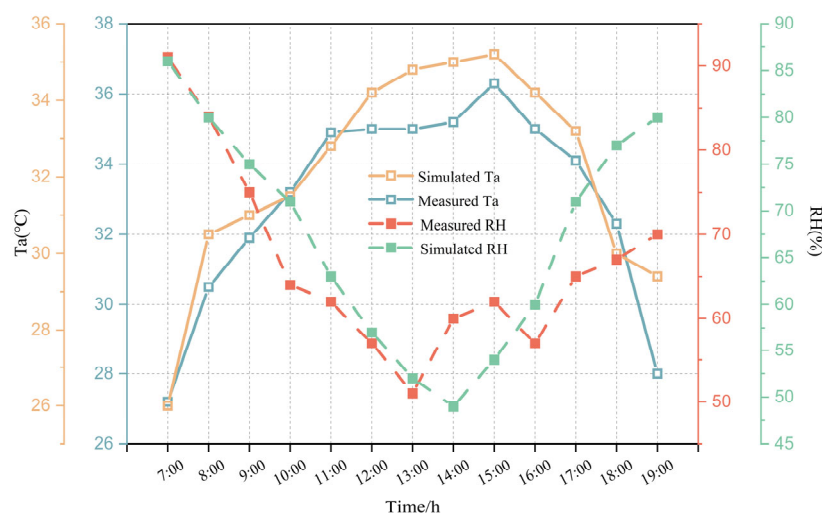
**Figure 4.** Sample point 3. Two-dimensional diagram and Model underlay surface material.

### 3.3. ENVI-Met Value Selection

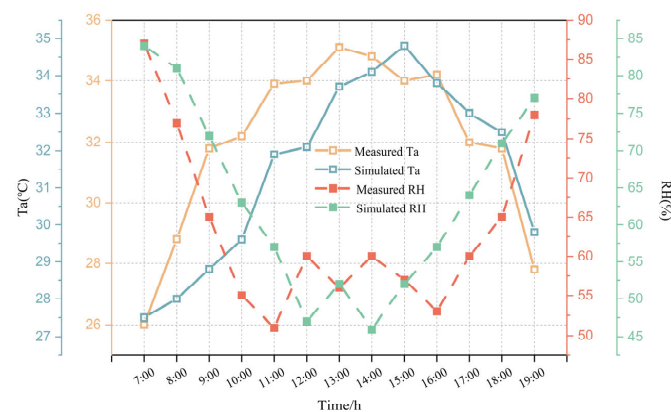
Measurements at the three sampling sites on July 8 showed a difference in  $T_a$  of 3 °C at the same time across different sites, with a peak between 14:00 and 16:00 and the fastest  $T_a$  drop after 17:00. Overall, sample point 1 exhibited a higher  $T_a$  bias, followed by sample sites 3 and 2. Notably, the change in relative humidity was opposite to the observed  $T_a$  trend. Humidity was the highest at sample point 2, which was closer to the water body. At sample point 1, the humidity was at its lowest at 13:00. Our field measurements were validated against simulated data. Our analysis showed that the simulated and measured  $T_a$  and humidity trends were approximately the same (Figures 5–7). This validated the reliability of the software for modeling the outdoor spaces of traditional villages.

Considering that ENVI-met software cannot be used to model the entire summer season, we chose a typical summer day as a representative of the summer meteorological characteristics. Through the screening of meteorological data, the simulation date of 8 July 2022 was selected as a typical summer day.

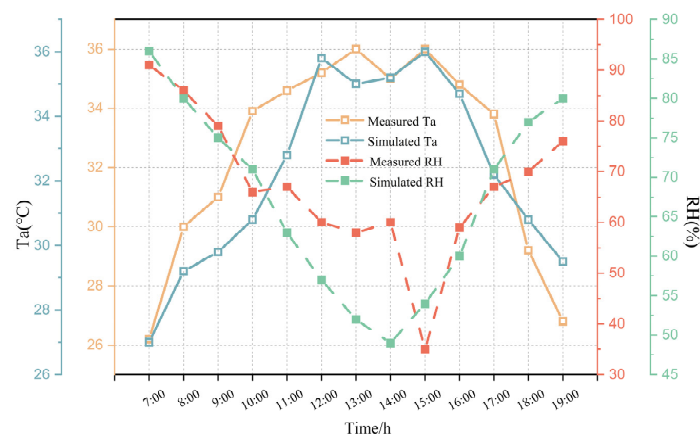
The ENVI-met software cannot be used to simulate the entire summer season; therefore, 8 July 2022 was chosen as the study date for the summer season because the meteorological parameters were most similar to the weather-station data. The meteorological data of this typical day were used as input parameters to simulate the environmental conditions of outdoor space in the core area of traditional villages and the thermal comfort distribution of three different types of outdoor space. The relevant meteorological data of the simulation day were determined by screening the meteorological data of a typical meteorological month in Chizhou City.



**Figure 5.** Sample point 1. Comparison of the measured and simulated data of  $T_a$  and relative humidity.



**Figure 6.** Sample point 2. Comparison of the measured and simulated data of Ta and relative humidity.



**Figure 7.** Sample point 3. Comparison of the measured and simulated data of Ta and relative humidity.

As Chizhou City belongs to the Cfa climate zone, with a long summer time, hot weather, and an extremely harsh thermal environment, we chose a typical summer day as a representative of the summer climate characteristics [28,29]. The study date for the summer season chosen was 8 July 2022 because the meteorological parameters were most similar to the weather-station data. The meteorological data of this typical day were used as input parameters to simulate the environmental conditions of outdoor space in the core areas of traditional villages and the thermal comfort distribution of three different types of outdoor space, and put forward the improvement strategy if the typical day can be improved; then, the thermal comfort in other times of summer will also have different degrees of improvement. The relevant meteorological data of the simulation day were determined by screening the meteorological data of a typical meteorological month in Chizhou City.

This study uses climate data from the National Centers for Environmental Information <https://www.ncei.noaa.gov/> (accessed on 2 February 2023). Weather-station data for the study date in Shimengao Village, including hourly Ta and relative humidity for 24 h, were obtained from a relevant weather-data website. Initial meteorological parameters were entered into the corresponding software interface as the base conditions for the simulation and the first hour was used as the warmup phase of the experiment (Tables 3 and 4).

**Table 3.** Initial meteorological parameters.

Total Initial Time Duration	Initial Temperature	Ws	Wd	RH	Roughness
07:00 (14 h)	20 °C	1.5 m/s	180°	Highest point 94%; Lowest point 31%	0.1



**Table 4.** Ta and RH data.

Time	Ta	RH	Time	Ta	RH	Time	Ta	RH
00:00	22.3 °C	88%	08:00	27.2 °C	58%	16:00	33.0 °C	31%
01:00	22.3 °C	83%	09:00	28.9 °C	51%	17:00	32.0 °C	36%
02:00	21.0 °C	88%	10:00	28.9 °C	51%	18:00	31.0 °C	40%
03:00	21.0 °C	88%	11:00	30.0 °C	45%	19:00	27.8 °C	54%
04:00	21.0 °C	83%	12:00	31.0 °C	43%	20:00	27.2 °C	58%
05:00	20.0 °C	94%	13:00	32.2 °C	36%	21:00	25.0 °C	69%
06:00	22.3 °C	83%	14:00	33.0 °C	38%	22:00	23.9 °C	78%
07:00	23.9 °C	78%	15:00	33.0 °C	31%	23:00	22.8 °C	88%

### 3.4. Outdoor Thermal Comfort Calculation

Thermal comfort refers to subjective perceptions of the external environment [30]. The physiologically equivalent Ta is more universal and mature than the outdoor space thermal comfort evaluation index and is suitable for mesoscale spatial simulations. Therefore, the PET was selected in this study to quantitatively analyze the thermal comfort of outdoor spaces in the core area of traditional village integration and three different types of outdoor spaces. The following equation was used [31]:

$$M + C + R + W + S + E_D + E_{Re} + E_{Sw} = 0 \quad (1)$$

where  $M$  represents the metabolic rate of the body,  $C$  is the convective heat flow,  $R$  represents the net body radiation,  $W$  is the external work,  $S$  represents body-heat storage,  $E_D$  is the latent heat flow due to water-vapor diffusion,  $E_{Re}$  is the heat exchange due to respiration, and  $E_{Sw}$  represents the heat flow due to sweat evaporation.

The climatic environment of different regions affects the subjective perception of human thermal comfort, with different thermal comfort sensations being also applicable to different thermal sensation intervals [32–34]. A thermal comfort class range classification based on the Köppen climate classification, which was employed in the study by Liu of over 700 test sites in Changsha [35], was used to analyze outdoor thermal comfort in this study. Both the study area and Changsha belong to the Cfa climate zone. Therefore, the PET range of outdoor thermal comfort in Changsha was used in this study as the standard for evaluating the thermal comfort of outdoor spaces in traditional villages (Table 5).

**Table 5.** Classification of PET value levels and ranges.

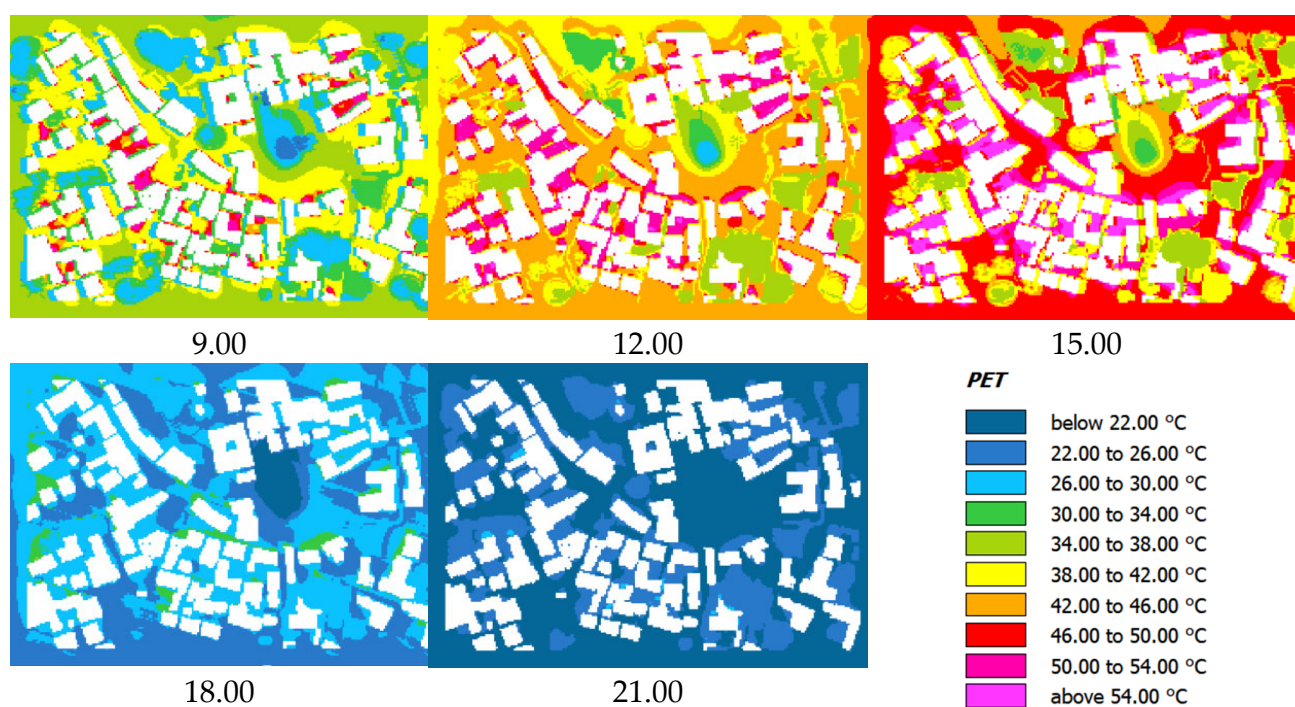
Thermal Sensation	Very Cold	Cold	Cool	Slightly Cool	Neutral	Slightly Warm	Warm	Hot	Very Hot
PET (°C)	<−8	−8~−1	−1~7	7~15	15~22	22~30	30~38	38~46	>46

## 4. Results and Analysis

In this study, we modeled and simulated the outdoor space in the core area of traditional village integration and three different types of outdoor spaces using the ENVI-core plugin. In particular, we calculated and analyzed the thermal comfort values of these spaces using the BIO-met correlation plugin. We selected five whole time points at 3 h intervals during the summer study dates and used a human height of 1.4 m as the observation height to determine the spatiotemporal distribution of thermal comfort in the abovementioned spaces and the spatial proportion of human comfort in different outdoor spaces during summer in order to identify spaces with poor thermal comfort. In addition, we identified the factors influencing thermal comfort in outdoor spaces in traditional villages. These results can be used to propose localized strategies for improving thermal comfort in such areas.

#### 4.1. Spatiotemporal Distribution of Thermal Comfort in the Core Area of Traditional Village Integration during Summer

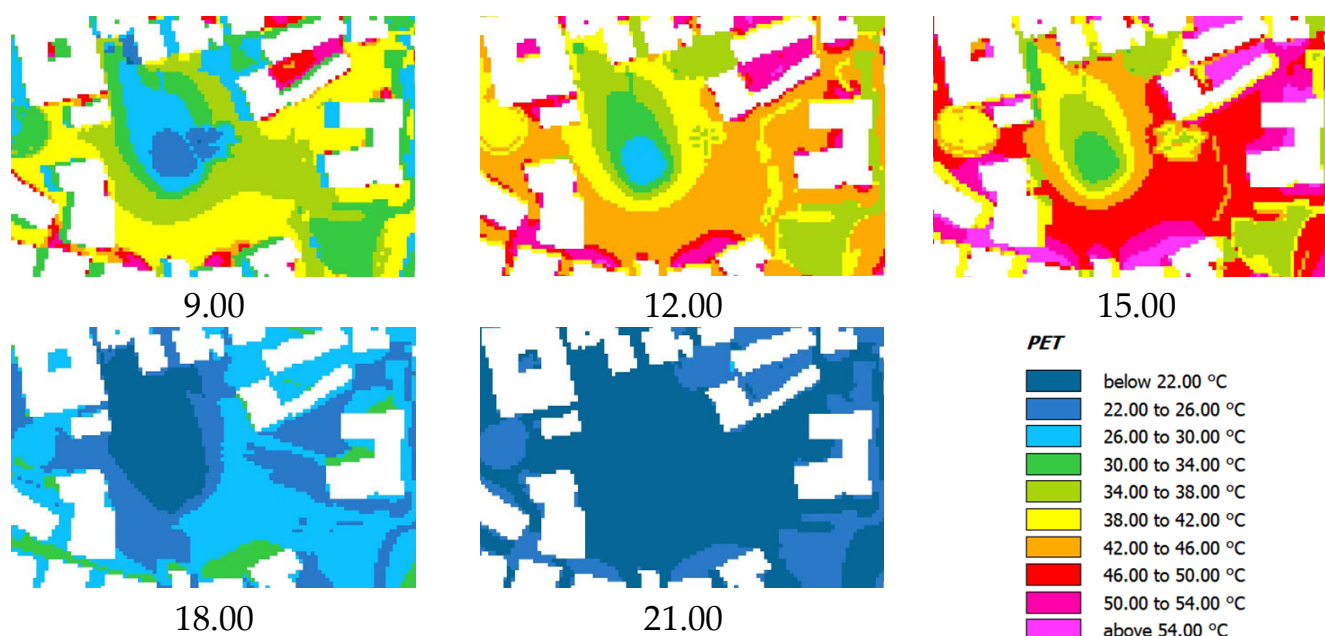
The distribution of human comfort in the outdoor spaces of traditional villages in the core area of integration showed that the overall PET was low and the thermal comfort of these spaces was good at 9:00 on the study day. As shown in Figure 8, the dark-blue areas are located near the squares, with most blue areas being close to waterbodies or in spaces in which buildings and trees provide shade. We found that their PET values ranged from 26 to 30 °C, corresponding to a “slightly warm” thermal comfort level. The yellow areas, which are mostly located in street spaces, exhibited a range of PET values of 38 to 42 °C, corresponding to a “hot” thermal comfort level. We also determined that orange, red, and purple areas, which are mostly located in areas with a high building density and poor ventilation, had PET values above 42 °C, corresponding to “hot” and “very hot” thermal comfort ratings. We also observed that at 12:00 on the study day, the overall PET value was slowly increasing compared with that at 9:00. The thermal comfort level was “hot” and “very hot” in most areas with high building density. As yellow and red areas are surrounded by many buildings, ventilation in these areas is difficult. Consequently, these areas with poor air circulation exhibited high PET values. We noticed that, in some areas, the thermal comfort was better in spaces close to water bodies and planted landscapes. We observed that, at 15:00, red areas started to increase in size, with more of them being observed in spaces with obstructed air circulation. Yellow and red areas had PET values > 38 °C, corresponding to a thermal comfort level of “very hot”; that is, the worst thermal comfort level. Staying in such an area for long periods can cause discomfort to the human body. However, we detected that, at 18:00, the overall PET values had significantly decreased. More specifically, we found that the PET values in sky-blue and blue areas mainly ranged between 24 and 30 °C, corresponding to a thermal comfort level of “slightly warm”, due to the fact that outdoor ground materials dissipated heat more quickly, cooling down the  $T_a$  and improving the thermal comfort in a summer day. At 21:00, the overall PET values were approximately the same across all areas; that is, the difference in the basic thermal comfort level was insignificant (Figure 8).



**Figure 8.** Spatiotemporal distribution of PET values on a summer day.

#### 4.2. Spatiotemporal Distribution of Thermal Comfort in Plaza Spaces

We observed that, at 9:00, the overall thermal comfort level was mostly in the yellow zone, with PET values ranging from 38 to 42 °C, corresponding to a thermal comfort level of “hot”. We noticed that areas with higher thermal comfort levels than the yellow zone were mostly located further away from the square and the central waterbody; that is, near residential areas with a higher building density and obstructed ventilation. We identified that more suitable areas were located near central physical landscapes, with PET values of <30 °C, corresponding to a thermal comfort level of “slightly warm” and “neutral”. At 12:00, we detected that the overall thermal comfort level was increased compared with that in the morning, being overall in the orange zone with a range of PET values of 42–46 °C, corresponding to a “hot” thermal comfort rating. We also detected a small number of areas with higher thermal comfort levels that were located in the nonshaded areas of buildings. We noticed that the thermal comfort levels were higher in the immediate vicinity of buildings compared with those in most plaza spaces. In particular, they were higher in spaces away from buildings because of the obstructed ventilation and lack of shading from buildings. At 15:00, the overall thermal comfort level was increased to its daily maximum. As shown in Figure 9, most areas are red, with PET values of 46–50 °C, corresponding to a thermal comfort level of “very hot”. We determined that the formation of shaded areas on the southern and eastern sides of buildings is difficult because of the movement of the sun and lack of ventilation, hindering the reduction in the original thermal  $T_a$ , while creating a closed and hot environment, whereas small yellow areas are located on the east side of buildings due to building shading. We found that, at 18:00, the overall  $T_a$  significantly dropped by 20 °C due to the openness of the square and the faster wind speed in the afternoon. However, we still observed several blue areas retaining the original higher thermal comfort level, corresponding to the “warm” level, whereas the thermal comfort level in the rest areas was mostly “slightly warm”. By 21:00, the basic thermal comfort levels differed insignificantly, exhibiting approximately similar PET values (Figure 9).

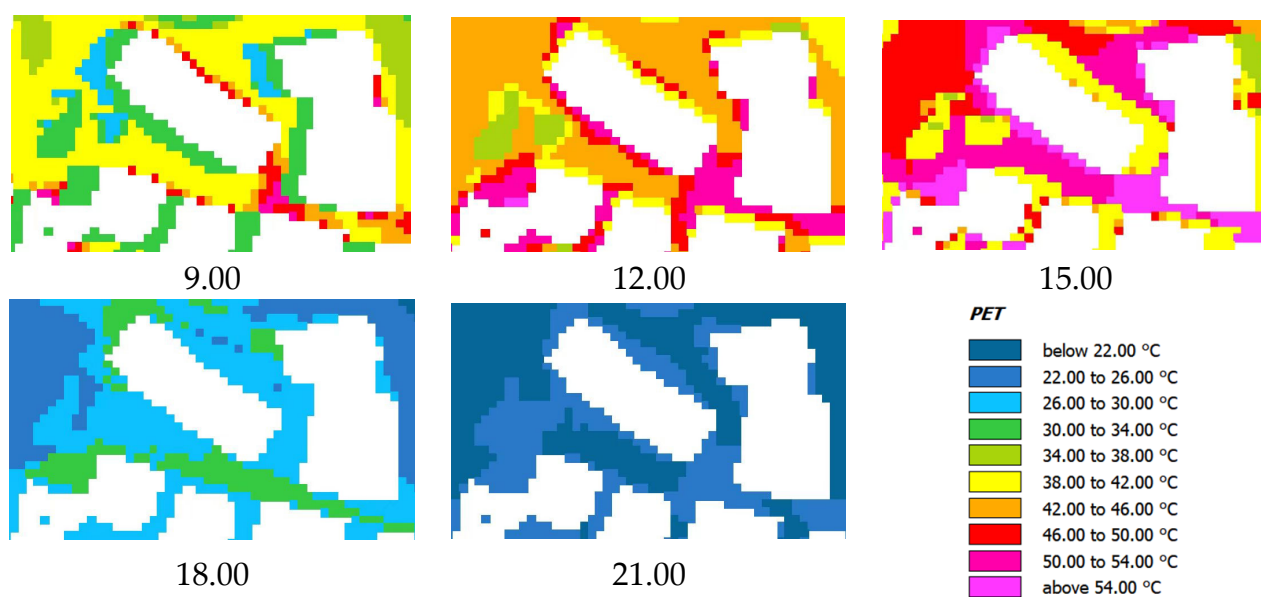


**Figure 9.** Spatiotemporal distribution of PET values in the square space on a summer day.

#### 4.3. Analysis of the Thermal Comfort of the Street Space

We found that the overall thermal comfort level at 9:00 was mainly in the yellow zone, with PET values ranging from 38 to 42 °C, corresponding to a “hot” thermal comfort level. As shown in Figure 10, red areas, which have a higher thermal comfort level than yellow areas, are mostly located near buildings on both sides of the street. Due to the angle of the

sun and building height, the formation of large shaded areas by buildings is not possible at this time. At 12:00, the overall thermal comfort level was significantly increased compared with that in the morning, being in the orange zone with a range of PET values of 42–46 °C, corresponding to a “very hot” thermal comfort level. Compared with the plaza site at 12:00, we noticed that the PET values increased faster due to the high building density, which resulted in a lower wind speed in the street space, preventing heat dissipation and creating a poor thermal environment [36]. However, we found fewer orange areas located near fences in the streets and alleys, indicating that external facilities increase thermal comfort. At 15:00, the overall thermal comfort level of the street space reached the daily maximum. Accordingly, most areas are purple–pink, with PET values ranging from 54 °C upwards, corresponding to a thermal comfort level of “very hot”. Interestingly, the southern and eastern sides of buildings in the alleyway exhibited the same level of thermal comfort due to the shading provided by the buildings. However, we detected a small number of red and yellow areas, mainly around village buildings, which provide shade. At 18:00, the overall  $T_a$  significantly dropped by 20 °C. We also determined that, compared with the square site, the street space exhibited a slower cooling rate, especially in green areas in which PET values ranged from 34 to 37 °C, corresponding to a “warm” thermal comfort level. At 21:00, the overall PET values were more or less the same, with the  $T_a$  dropping below 26 °C (Figure 10).



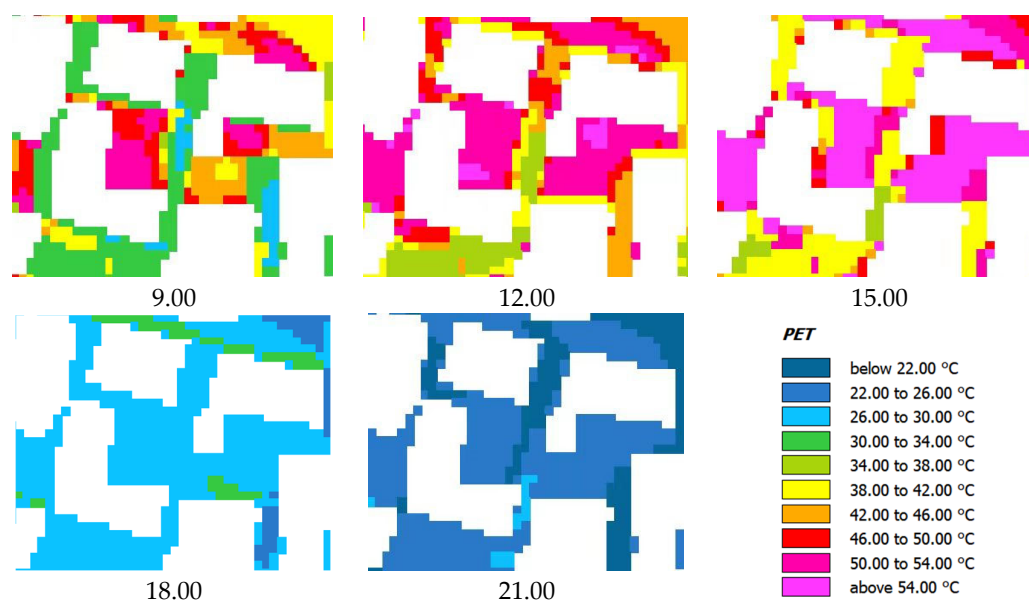
**Figure 10.** Spatiotemporal distribution of PET in Old Street and Lane Space on a summer day.

#### 4.4. Analysis of the Thermal Comfort of the Courtyard Space

We observed that, at 9:00, the overall thermal comfort level was low in the center, whereas it was high in the surroundings. Most areas were in the orange zone, with PET values ranging from 42 to 54 °C, corresponding to a “very hot” thermal comfort level. As shown in Figure 11, areas with a higher thermal comfort level are mostly located on the west side of the building, with PET values of >50 °C, corresponding to a “very hot” thermal comfort level. This was attributed to the high thermal environment caused by the direct sunlight and the absence of any shade. In contrast, areas with a more favorable thermal comfort level are located in small interstices between the buildings, as they receive shading from buildings, and appear as green areas with PET values ranging from 42 to 46 °C, corresponding to a “hot” thermal comfort level. At 12:00, the overall thermal comfort level increased more rapidly than that in the morning, forming purple and pink areas with PET values of 50 °C and above, corresponding to a “very hot” thermal comfort level. We also detected a small number of areas with higher thermal comfort levels being located



in more enclosed spaces within the building envelope, with PET values reaching over 54 °C. Due to the obstructed ventilation of the courtyard space and the poor conditions, its thermal comfort level is very uncomfortable [37]. At 15:00, the courtyard space was “extremely hot”, with its largest proportion being in the purple zone. We observed that areas with lower thermal comfort levels were located on the northeastern sides of buildings, in the building shadow. The PET values ranged from 38 to 42 °C, corresponding to a “hot” thermal comfort level. At 18:00, the overall thermal comfort level decreased, with the corresponding PET value dropping below 34 °C. In particular, we detected that the PET values for the courtyard ranged from 26 to 34 °C, corresponding to a “slightly warm” thermal comfort level. Hence, the thermal environment was relatively comfortable. At 21:00, we noticed that the overall area was in the dark-blue zone, with the PET values dropping below 26 °C, corresponding to a thermal comfort rating of “slightly warm” and “neutral”. Hence, the overall thermal environment was relatively pleasant. Interestingly, we noticed that the area with the lowest thermal comfort rating was located in the middle of the open courtyard because of the high wind speed and lack of shade from buildings, which reduced the  $T_a$  more quickly (Figure 11).



**Figure 11.** Spatiotemporal distribution of PET in courtyard space on a summer day.

### 5. Strategies for Optimizing Thermal Comfort in Outdoor Spaces in the Shimengao Village

The results of the ENVI-met thermal comfort analysis for different spaces revealed that the thermal comfort in the Shimengao Village correlated with the overall spatial layout of the traditional village, external facilities of buildings, microlandscape settings, and outdoor ground materials. More specifically, the PET values corresponding to the outdoor spaces of the traditional village were increased until the afternoon on a summer day, when the thermal comfort worsened. Subsequently, these PET values began to decrease, improving the thermal comfort level of these spaces. Three different types of spaces were ranked from best to worst in terms of thermal comfort: square, street, and courtyard spaces (Table 6). Based on the abovementioned analysis of the thermal comfort environment in the Shimengao Village, we proposed a thermal comfort improvement strategy suitable for the traditional village according to its overall spatial layout, external building facilities, microlandscape settings, and outdoor-space materials.

**Table 6.** Thermal comfort level at different times in sample points 1–3 and the reasons for the difference in comfort levels among the sample points.

Location	Time	Main PET	Reasons
Sample point 1	09:00	26.0–42.0 °C	The square space has an open space and water body, which provide good thermal comfort. Thus, reasonable space layout and microlandscape settings enhance thermal comfort.
Sample point 2		38.0–42.0 °C	
Sample point 3		42.0–50.0 °C	
Sample point 1	12:00	34.0–46.0 °C	With the increase in Ta, the overall thermal comfort was reduced, whereas the thermal comfort under the shadow of buildings was increased. Since the square space is located in the tuiyue, the wind speed was higher, thus improving the thermal comfort in this space compared with that in other spaces.
Sample point 2		42.0–50.0 °C	
Sample point 3		50.0–54.0 °C	
Sample point 1	15:00	38.0–50.0 °C	The courtyard space exhibited poor thermal comfort because of a lack of ventilation.
Sample point 2		50.0–54.0 °C	
Sample point 3		>54.0 °C	
Sample point 1	18:00	22.0–30.0 °C	Compared with the street, the courtyard space was shaded by the surrounding buildings, exhibiting better thermal comfort.
Sample point 2		26.0–34.0 °C	
Sample point 3		26.0–30.0 °C	
Sample point 1	21:00	<22.0 °C	The drop in Ta resulted in a neutral thermal comfort across the whole area.
Sample point 2		22.0–26.0 °C	
Sample point 3		22.0–26.0 °C	

### 5.1. Optimization of the Spatial Layout of Traditional Villages to Improve Their Thermal Comfort

Improving the thermal comfort of areas in the Shimengao Village can be achieved by opening up skylights, combining alleyways, and managing the water system for optimizing the spatial layout of the village. However, the spatial layout of the Shimengao Village must be upgraded without destroying its architecture and character, which must be protected and preserved [38,39]. The more compact the layout of a building, the less heat it loses, and the higher the Ta [40]. At present, the building density in traditional villages can, to a certain extent, be reduced by opening up skylights. This mainly involves the conversion of certain auxiliary rooms and illegally built modern buildings inside the village to outdoor openings, such as gardens and squares, thus improving thermal comfort [41–43]. A combination of alleyways will also improve the flow of roads and provide orderly connections, resulting in improved ventilation inside the village, thus improving thermal comfort. Although the street space was better among the three types of examined spaces in terms of thermal comfort, it can still be improved by widening. The water system is mainly cleared from open ditches and culverts. In addition, street and square spaces were more comfortable than courtyard spaces because of the presence of ponds in square spaces and culverts, respectively. Water systems reduce the Ta and provide a certain level of humidity [8,44]. Water is also characterized by evaporative cooling, which reduces the hot Ta in the surrounding areas. Ponds and ditches can be upgraded to increase the water-friendly space and lower the Ta [45]. This will not only ensure the harmonization of the traditional village style and optimize its overall spatial layout but will also increase the wind speed, reduce the Ta in the summer, and improve the thermal comfort throughout the village.

### 5.2. Increase in External Building Amenities to Improve Thermal Comfort

For traditional villages, such as Shimengao, architectural optimization can be achieved by increasing the external facilities of buildings to provide building shadows, increase the wind speed, reduce PET values, and improve the thermal comfort of the traditional village. The buildings in Shimengao Village are mostly two-entry and two-compartment buildings, with the entire dwelling dominated by a patio. Traditional building shading includes four main types: roof, window, wall, and green shading. Thermal comfort is highly correlated with plant distribution [46,47] when combined with traditional building shading, such as by setting shading panels on the eaves [48] and windows and adding vine plants climbing the building walls. In plaza spaces, shades are added to public spaces, such as kiosks, providing a space for visitors and residents to relax and interact [49]. Street spaces can be shaded with canopies and advertising clothes. Traditional advertising

fabric provides shade, reducing the direct sunlight and enhancing the image of the street space and commercial vitality. In the courtyard space, which was the less comfortable outdoor space across all examined village spaces, thermal comfort can be improved by adding vertical vegetation and grapevines to reduce the  $T_a$  while maintaining the original residential texture [50].

### 5.3. Creation of Outdoor “Micro-Landscapes” to Improve Thermal Comfort

Thermal comfort in the outdoor spaces of traditional villages can be improved by creating various outdoor “micro-landscapes”. In the case of traditional villages, microlandscape optimization can be achieved by creating small gardens according to local conditions. These small gardens might include vegetables, bamboo, tea, or fruit gardens. This can be achieved by exploiting the unused land in front of houses, thus transforming the rural features. Small orchards and small bamboo gardens can also be added to squares to improve thermal comfort. Small orchards and bamboo gardens can be created by planting different types of plants to increase the shaded area and, thus, reduce the local  $T_a$  [51–56]. Small vegetable gardens, small gardens, and small tea gardens have low-growing plants that provide a degree of evaporating moisture, reducing the PET value of outdoor spaces [57–59]. Creating small vegetable gardens and small gardens in streets and courtyards will beautify the traditional village landscape and improve the quality of life of villagers. More importantly, the creation of microlandscape small gardens will improve the overall outdoor space thermal comfort of traditional villages, enable the full use of land resources, and increase the income of farmers without damaging the overall appearance of the landscape of traditional villages [41,60].

### 5.4. Changing the Materials of Outdoor Spaces to Improve Thermal Comfort

The use of highly reflective and insulating outdoor-space materials can reduce the  $T_a$  and improve thermal comfort. Different outdoor-space materials have different specific heat capacities and reflectivities. The surface temperatures of different outdoor-space materials differ, affecting the local  $T_a$  of the space above through air conduction [61]. Two main types of materials are used in outdoor spaces: (1) soft materials, mainly grass and other related vegetation, and (2) hard materials including building roofs, facades, and floor coverings. In courtyards and street spaces, thermal comfort can be improved by adding soft materials [62]. However, the materials to be used in outdoor spaces must match the traditional village style; for instance, hard materials must be selected from the local hard materials found in the area. Local vernacular materials, such as old bricks, tiles, and stones, must be fully utilized in architectural optimization. In terms of paving, it is necessary to choose stone paving materials that are in line with the traditional local village style for outdoor spaces. Sunlight can be reflected due to a higher ground reflectivity, thus reducing the absorption of sunlight and lowering the local  $T_a$  [63]. In addition, permeable materials can be used to absorb water from the air. When the external  $T_a$  reaches a certain level, the humidity of the air can be increased through evaporation, thus improving the thermal comfort of outdoor spaces of traditional villages [64].

## 6. Conclusions

In this study, the ENVI-met analysis software was used to study the thermal comfort of three outdoor spaces in the Shimengao Village, Tangxi Town. Analyses and simulations were conducted to optimize the overall spatial layout of traditional villages, increase the external facilities of buildings, create “micro-landscapes”, and change the materials of outdoor spaces. The results of this study were used to improve the thermal comfort of the traditional village of Shimengao. They can also be applied to other traditional villages in typical mountainous areas of southern Anhui to achieve conservation and sustainable development.

This study selected the traditional Shimengao village as the research object and 8 July 2022, as the actual measurement date. Depthmap software was used to identify the

area in the traditional village that is most frequently used by villagers and tourists as the research area, while the ENVI-met analysis software was used to simulate the integration core area and thermal comfort distribution of three types of outdoor spaces in the Shimengao Village. The factors affecting thermal comfort were analyzed and the strategies to improve the thermal comfort of traditional villages were determined by taking into consideration local characteristics. The main conclusions were as follows.

(1) Basic data on the outdoor-space environment of the Shimengao Village were obtained and measured. Meteorological data of  $T_a$  and humidity in the traditional village were obtained in regular intervals and the microclimate of each site was analyzed in the early stage based on these data. Space syntax theory was used to identify the core area of traditional village integration and determine three typical outdoor spaces; that is, square, street, and courtyard spaces.

(2) The thermal comfort of the traditional village integration core area and three types of outdoor space were analyzed to mechanistically explore the effect of thermal comfort. On a summer day, the PET value in the core area of the traditional village reached its peak at 15:00, followed by a downward trend, resulting in a relatively suitable thermal environment. From the perspective of an entire day, thermal comfort was better near shaded areas, water bodies, and plant landscapes. The PET values of open areas, where thermal comfort is better, were higher. During summer, the thermal environment of each space was poor throughout the day, with the thermal comfort level being the worst at 15:00, exceeding the grade of “very hot.” Three different types of spaces were ranked from best to worst in terms of thermal comfort: square, street, and courtyard spaces. The square space exhibited the highest level of thermal comfort due to its rate of green lands and water bodies, whereas the courtyard space, which is relatively closed and lacks a smooth air circulation, had the lowest level of thermal comfort.

(3) The degree and mechanism of influence of different climate factors on thermal comfort were analyzed and improvement strategies were proposed based on improving the thermal comfort of outdoor spaces, including optimizing the overall spatial layout of traditional villages, adding external facilities in buildings, creating “micro-landscapes,” and changing the materials of outdoor spaces.

The results of this study can provide a reference for improving thermal comfort in other traditional villages; however, this study has some limitations. First, only the measured data and simulation of typical summer days were selected in this study and, as such, actual measurements and simulations of other months are lacking. Second, because of the limitations of the simulation software and computer performance, only the core area of traditional village integration was simulated, whereas the whole traditional village was not studied. Finally, microclimate plays an important role in tourist activities and the influence of climate variables on thermal comfort should be further considered in external studies [65]. Therefore, the scope and depth of research should be expanded in future studies, so as to strengthen the research on the thermal comfort of traditional villages.

**Author Contributions:** Methodology, L.S. and S.Z.; software, L.S. and L.Z.; validation, L.S. and S.Z.; formal analysis, L.S.; investigation, T.X.; resources, T.X.; data curation, T.X.; writing—original draft preparation, L.S.; writing—review and editing, T.X. and L.S.; visualization, S.Z.; supervision, T.S.; project administration, T.X.; funding acquisition, T.X. All authors have read and agreed to the published version of the manuscript.

**Funding:** This research was funded by Anhui Provincial Department of Education Major Project (SK2020ZD25), Anhui Province Housing and Urban–Rural Construction Science and Technology Program (2022-RK035), Key Projects of Humanities and Social Science Foundation of the Anhui Higher Education Institutions of China (2022AH050226) and Open Subjects of Research Platform of Prefabricated Building Research Institute of Anhui Province (AHZPY2021ZR02).

**Institutional Review Board Statement:** Not applicable, for research that does not involve humans.

**Informed Consent Statement:** Informed consent has been obtained from all subjects participating in the study.



**Data Availability Statement:** Publicly available datasets were analyzed in this study. These data can be found on the Anhui Meteorological Bureau.

**Conflicts of Interest:** There are no conflict of interest.

### Abbreviations

PET	Physiological equivalent temperature (°C);
RH	Relative humidity (%);
Ta	Air temperature (°C);
Wd	Wind direction (°);
Ws	Wind speed (m/s)

### References

1. Zhen, M.; Dong, Q.; Chen, P.; Ding, W.; Zhou, D.; Feng, W. Urban outdoor thermal comfort in western China. *J. Asian Archit. Build. Eng.* **2021**, *20*, 222–236. [\[CrossRef\]](#)
2. Guo, Q.; Liu, X.X. Evaluation and Optimization Design for Microclimate Comfort of Traditional Village Squares Based on Extension Correlation Function. *J. Environ. Public Health* **2022**, *2022*, 6106463. [\[CrossRef\]](#) [\[PubMed\]](#)
3. Perini, K.; Chokhachian, A.; Dong, S.; Auer, T. Modeling and simulating urban outdoor comfort: Coupling ENVI-Met and TRNSYS by grasshopper. *Energy Build.* **2017**, *152*, 373–384. [\[CrossRef\]](#)
4. Guo, T.Y.; Zhao, Y.; Yang, J.H.; Zhong, Z.N.; Ji, K.F.; Zhong, Z.Y.; Luo, X.Y. Effects of Tree Arrangement and Leaf Area Index on the Thermal Comfort of Outdoor Children’s Activity Space in Hot-Humid Areas. *Buildings* **2023**, *13*, 214. [\[CrossRef\]](#)
5. Tsoka, S.; Tsikaloudaki, A.; Theodosiou, T. Analyzing the ENVI-met microclimate model’s performance and assessing cool materials and urban vegetation applications-A review. *Sustain. Cities Soc.* **2018**, *43*, 55–76. [\[CrossRef\]](#)
6. Gadish, I.; Saaroni, H.; Pearlmutter, D. A predictive analysis of thermal stress in a densifying urban business district under summer daytime conditions in a Mediterranean City. *Urban Clim.* **2023**, *48*, 101298. [\[CrossRef\]](#)
7. Xu, M.; Hong, B.; Mi, J.Y.; Yan, S.S. Outdoor thermal comfort in an urban park during winter in cold regions of China. *Sustain. Cities Soc.* **2018**, *43*, 208–220. [\[CrossRef\]](#)
8. Cheng, Y.Y.; Liu, X.; Zeng, Z.; Liu, S.S.; Wang, Z.Y.; Tang, X.; He, B.J. Impacts of Water Bodies on Microclimates and Outdoor Thermal Comfort: Implications for Sustainable Rural Revitalization. *Front. Environ. Sci.* **2022**, *10*, 940482. [\[CrossRef\]](#)
9. Han, J.; Li, X.Y.; Li, B.Y.; Yang, W.; Yin, W.; Peng, Y.; Feng, T. Research on the influence of courtyard space layout on building microclimate and its optimal design. *Energy Build.* **2023**, *289*, 113035. [\[CrossRef\]](#)
10. Morakinyo, T.E.; Lam, Y.F. Simulation study on the impact of tree-configuration, planting pattern and wind condition on street-canyon’s micro-climate and thermal comfort. *Build. Environ.* **2016**, *103*, 262–275. [\[CrossRef\]](#)
11. Deng, W.; Xia, C.H.; Chen, J.Y.; Jiang, Y.J. An Examination of the Thermal Comfort Impacts of Ficus altissima on the Climate in Lower Subtropical China during the Winter Season. *Sustainability* **2023**, *15*, 2427. [\[CrossRef\]](#)
12. Thomas, G.; Thomas, J.; Mathews, G.M.; Alexander, S.P.; Jose, J. Assessment of the potential of green wall on modification of local urban microclimate in humid tropical climate using ENVI-met model. *Ecol. Eng.* **2023**, *187*, 106868. [\[CrossRef\]](#)
13. Lopes, H.S.; Remoaldo, P.C.; Ribeiro, V.; Martín-Vide, J. Perceptions of human thermal comfort in an urban tourism destination—A case study of Porto (Portugal). *Build. Environ.* **2021**, *205*, 108246. [\[CrossRef\]](#)
14. Xin, K.; Zhao, J.Y.; Wang, T.H.; Gao, W.J. Supporting Design to Develop Rural Revitalization through Investigating Village Microclimate Environments: A Case Study of Typical Villages in Northwest China. *Int. J. Environ. Res. Public Health* **2022**, *19*, 8310. [\[CrossRef\]](#)
15. Fan, Q.D.; Du, F.T.; Li, H.; Zhang, C.M. Thermal-comfort evaluation of and plan for public space of Maling Village, Henan, China. *PLoS ONE* **2021**, *16*, e0256439. [\[CrossRef\]](#)
16. Yang, S.Q.; Matzarakis, A. Implementation of human thermal comfort and air humidity in Koppen-Geiger climate classification and importance towards the achievement of Sustainable Development Goals. *Theor. Appl. Climatol.* **2019**, *138*, 981–998. [\[CrossRef\]](#)
17. Wang, H.F.; Chiou, S.C. Study on the Sustainable Development of Human Settlement Space Environment in Traditional Villages. *Sustainability* **2019**, *11*, 4186. [\[CrossRef\]](#)
18. Jiang, Y.J.; Li, N.; Wang, Z.Y. Parametric Reconstruction of Traditional Village Morphology Based on the Space Gene Perspective—The Case Study of Xiaoxi Village in Western Hunan, China. *Sustainability* **2023**, *15*, 2088. [\[CrossRef\]](#)
19. Xiang, H.W.; Qin, Y.; Xie, M.J.; Zhou, B. Study on the “Space Gene” Diversity of Traditional Dong Villages in the Southwest Hunan Province of China. *Sustainability* **2022**, *14*, 14306. [\[CrossRef\]](#)
20. Askarizad, R.; Safari, H. Investigating the role of semi-open spaces on the sociability of public libraries using space syntax (Case Studies: Sunrise Mountain and Desert Broom Libraries, Arizona, USA). *Ain Shams Eng. J.* **2020**, *11*, 253–264. [\[CrossRef\]](#)
21. Alalouch, C.; Al-Hajri, S.; Naser, A.; Al Hinai, A. The impact of space syntax spatial attributes on urban land use in Muscat: Implications for urban sustainability. *Sustain. Cities Soc.* **2019**, *46*, 101417. [\[CrossRef\]](#)
22. Lee, S.; Yoo, C.; Seo, K.W. Determinant Factors of Pedestrian Volume in Different Land-Use Zones: Combining Space Syntax Metrics with GIS-Based Built-Environment Measures. *Sustainability* **2020**, *12*, 8647. [\[CrossRef\]](#)
23. Li, R.; Mao, L. Spatial Characteristics of Suburban Villages Based on Spatial Syntax. *Sustainability* **2022**, *14*, 14195. [\[CrossRef\]](#)

24. Lopez-Cabeza, V.P.; Diz-Mellado, E.; Rivera-Gomez, C.; Galan-Marin, C.; Samuelson, H.W. Thermal comfort modelling and empirical validation of predicted air temperature in hot-summer Mediterranean courtyards. *J. Build. Perform. Simul.* **2022**, *15*, 39–61. [\[CrossRef\]](#)
25. Lopez-Cabeza, V.P.; Galan-Marin, C.; Rivera-Gomez, C.; Roa-Fernandez, J. Courtyard microclimate ENVI-met outputs deviation from the experimental data. *Build. Environ.* **2018**, *144*, 129–141. [\[CrossRef\]](#)
26. Abd Elraouf, R.; ELMokadem, A.; Megahed, N.; Eleinen, O.A.; Eltarabily, S. Evaluating urban outdoor thermal comfort: A validation of ENVI-met simulation through field measurement. *J. Build. Perform. Simul.* **2022**, *15*, 268–286. [\[CrossRef\]](#)
27. Liu, Z.H. Numerical Simulation Study of Microclimate in Urban Old Residential Transformation Area Based on Envi-Met Software. *Fresenius Environ. Bull.* **2022**, *31*, 11297–11304.
28. Kim, S.W.; Brown, R.D. Pedestrians' behavior based on outdoor thermal comfort and micro-scale thermal environments, Austin, TX. *Sci. Total Environ.* **2022**, *808*, 152143. [\[CrossRef\]](#)
29. Corchado, E.; Arroyo, A.; Tricio, V. Soft computing models to identify typical meteorological days. *Log. J. Igpl* **2011**, *19*, 373–383. [\[CrossRef\]](#)
30. Liu, C.; Tang, L.N.; Yan, J.S.; Ouyang, J.Y. Direct and indirect effects of multisensory modalities on visitor's thermal comfort in an urban park in a humid-hot climate. *Int. J. Sustain. Dev. World Ecol.* **2023**, *30*, 319–328. [\[CrossRef\]](#)
31. Blazejczyk, K.; Epstein, Y.; Jendritzky, G.; Staiger, H.; Tinz, B. Comparison of UTCI to selected thermal indices. *Int. J. Biometeorol.* **2012**, *56*, 515–535. [\[CrossRef\]](#)
32. Johansson, E.; Yahia, M.W.; Arroyo, I.; Bengs, C. Outdoor thermal comfort in public space in warm-humid Guayaquil, Ecuador. *Int. J. Biometeorol.* **2018**, *62*, 387–399. [\[CrossRef\]](#)
33. Yan, T.K.; Jin, Y.M.; Jin, H. Combined effects of the visual-thermal environment on the subjective evaluation of urban pedestrian streets in severely cold regions of China. *Build. Environ.* **2023**, *228*, 109895. [\[CrossRef\]](#)
34. Lai, D.Y.; Guo, D.H.; Hou, Y.F.; Lin, C.Y.; Chen, Q.Y. Studies of outdoor thermal comfort in northern China. *Build. Environ.* **2014**, *77*, 110–118. [\[CrossRef\]](#)
35. Liu, W.W.; Zhang, Y.X.; Deng, Q.H. The effects of urban microclimate on outdoor thermal sensation and neutral temperature in hot-summer and cold-winter climate. *Energy Build.* **2016**, *128*, 190–197. [\[CrossRef\]](#)
36. Zhou, J.Y.; Zhang, X.J.; Xie, J.C.; Liu, J.P. Effects of elevated air speed on thermal comfort in hot-humid climate and the extended summer comfort zone. *Energy Build.* **2023**, *287*, 112953. [\[CrossRef\]](#)
37. Lopez-Cabeza, V.P.; Rivera-Gomez, C.; Roa-Fernandez, J.; Hernandez-Valencia, M.; Herrera-Limones, R. Effect of thermal inertia and natural ventilation on user comfort in courtyards under warm summer conditions. *Build. Environ.* **2023**, *228*, 109812. [\[CrossRef\]](#)
38. Li, T.S.; Zhang, M.H.; Gu, X.G. Optimization strategies for conservation of traditional dwellings in Hongcun Village, China, based on decay phenomena analysis. *PLoS ONE* **2022**, *17*, e0276306. [\[CrossRef\]](#)
39. Chen, W.X.; Yang, L.Y.; Wu, J.H.; Wu, J.H.; Wang, G.Z.; Bian, J.J.; Zeng, J.; Liu, Z.L. Spatio-temporal characteristics and influencing factors of traditional villages in the Yangtze River Basin: A Geodetector model. *Herit. Sci.* **2023**, *11*, 111. [\[CrossRef\]](#)
40. Ma, K.; Tang, X.L.; Ren, Y.J.; Wang, Y.W. Research on the Spatial Pattern Characteristics of the Taihu Lake “Dock Village” Based on Microclimate: A Case Study of Tangli Village. *Sustainability* **2019**, *11*, 368. [\[CrossRef\]](#)
41. Xiong, Y.; Zhang, J.P.; Yan, Y.; Sun, S.B.; Xu, X.Y.; Higuera, E. Effect of the spatial form of Jiangnan traditional villages on microclimate and human comfort. *Sustain. Cities Soc.* **2022**, *87*, 104136. [\[CrossRef\]](#)
42. Tao, J.; Xiao, D.W.; Qin, Q.H.; Zhuo, X.L.; Wang, J.Y.; Chen, H.S.; Wang, Q. Climate-adaptive Design of Historic Villages and Dwellings in a Typhoon-prone Region in Southernmost Mainland China. *Int. J. Archit. Herit.* **2022**, *16*, 117–135. [\[CrossRef\]](#)
43. Johansson, E. Influence of urban geometry on outdoor thermal comfort in a hot dry climate: A study in Fez, Morocco. *Build. Environ.* **2006**, *41*, 1326–1338. [\[CrossRef\]](#)
44. Gou, S.Q.; Li, Z.R.; Zhao, Q.; Nik, V.M.; Scartezzini, J.L. Climate responsive strategies of traditional dwellings located in an ancient village in hot summer and cold winter region of China. *Build. Environ.* **2015**, *86*, 151–165. [\[CrossRef\]](#)
45. Coutts, A.M.; Tapper, N.J.; Beringer, J.; Loughnan, M.; Demuzere, M. Watering our cities: The capacity for Water Sensitive Urban Design to support urban cooling and improve human thermal comfort in the Australian context. *Prog. Phys. Geogr.-Earth Environ.* **2013**, *37*, 2–28. [\[CrossRef\]](#)
46. Li, Z.R.; Feng, X.W.; Sun, J.T.; Li, C.; Yu, W.X.; Fang, Z.S. STMRT: A simple tree canopy radiative transfer model for outdoor mean radiant temperature. *Build. Environ.* **2023**, *228*, 109846. [\[CrossRef\]](#)
47. Lai, D.Y.; Liu, Y.Q.; Liao, M.C.; Yu, B.Q. Effects of different tree layouts on outdoor thermal comfort of green space in summer Shanghai. *Urban Clim.* **2023**, *39*, 101398. [\[CrossRef\]](#)
48. Lopez-Cabeza, V.P.; Diz-Mellado, E.; Rivera-Gomez, C.A.; Galan-Marin, C. Shade and Thermal Comfort in Courtyards: Experimental versus Simulation Results. *Buildings* **2022**, *12*, 1961. [\[CrossRef\]](#)
49. Rossi, F.; Cardinali, M.; Di Giuseppe, A.; Castellani, B.; Nicolini, A. Outdoor thermal comfort improvement with advanced solar awnings: Subjective and objective survey. *Build. Environ.* **2022**, *215*, 108967. [\[CrossRef\]](#)
50. Zheng, B.H.; Li, J.Y.; Chen, X.; Luo, X. Evaluating the Effects of Roof Greening on the Indoor Thermal Environment throughout the Year in a Chinese City (Chenzhou). *Forests* **2022**, *13*, 304. [\[CrossRef\]](#)
51. Hosseinzadeh, A.; Bottacin-Busolin, A.; Keshmiri, A. A Parametric Study on the Effects of Green Roofs, Green Walls and Trees on Air Quality, Temperature and Velocity. *Buildings* **2022**, *12*, 2159. [\[CrossRef\]](#)

52. Hwang, R.L.; Lin, T.P.; Matzarakis, A. Seasonal effects of urban street shading on long-term outdoor thermal comfort. *Build. Environ.* **2011**, *46*, 863–870. [\[CrossRef\]](#)
53. Mohammad, P.; Aghlmand, S.; Fadaei, A.; Gachkar, S.; Gachkar, D.; Karimi, A. Evaluating the role of the albedo of material and vegetation scenarios along the urban street canyon for improving pedestrian thermal comfort outdoors. *Urban Clim.* **2021**, *40*, 100993. [\[CrossRef\]](#)
54. Morakinyo, T.E.; Kong, L.; Lau, K.K.L.; Yuan, C.; Ng, E. A study on the impact of shadow-cast and tree species on in-canyon and neighborhood's thermal comfort. *Build. Environ.* **2017**, *115*, 1–17. [\[CrossRef\]](#)
55. Zhang, L.; Zhan, Q.M.; Lan, Y.L. Effects of the tree distribution and species on outdoor environment conditions in a hot summer and cold winter zone: A case study in Wuhan residential quarters. *Build. Environ.* **2018**, *130*, 27–39. [\[CrossRef\]](#)
56. Yu, H.M.; Zhang, T.; Fukuda, H.; Ma, X. The effect of landscape configuration on outdoor thermal environment: A case of urban Plaza in Xi'an, China. *Build. Environ.* **2023**, *231*, 110027. [\[CrossRef\]](#)
57. Zhang, L.L.; Liu, H.R.; Wei, D.; Liu, F.; Li, Y.R.; Li, H.L.; Dong, Z.J.; Cheng, J.Y.; Tian, L.; Zhang, G.M.; et al. Impacts of Spatial Components on Outdoor Thermal Comfort in Traditional Linpan Settlements. *Int. J. Environ. Res. Public Health* **2022**, *19*, 6421. [\[CrossRef\]](#)
58. Simon, H.; Linden, J.; Hoffmann, D.; Braun, P.; Bruse, M.; Esper, J. Modeling transpiration and leaf temperature of urban trees—A case study evaluating the microclimate model ENVI-met against measurement data. *Landsc. Urban Plan.* **2018**, *174*, 33–40. [\[CrossRef\]](#)
59. Zaki, S.A.; Toh, H.J.; Yakub, F.; Saudi, A.S.M.; Ardila-Rey, J.A.; Muhammad-Sukki, F. Effects of Roadside Trees and Road Orientation on Thermal Environment in a Tropical City. *Sustainability* **2020**, *12*, 1053. [\[CrossRef\]](#)
60. Singh, M.K.; Mahapatra, S.; Atreya, S.K. Bioclimatism and vernacular architecture of north-east India. *Build. Environ.* **2009**, *44*, 878–888. [\[CrossRef\]](#)
61. Yang, X.S.; Zhao, L.H.; Bruse, M.; Meng, Q.L. Evaluation of a microclimate model for predicting the thermal behavior of different ground surfaces. *Build. Environ.* **2013**, *60*, 93–104. [\[CrossRef\]](#)
62. Yang, J.Y.; Hu, X.Y.; Feng, H.Y.; Marvin, S. Verifying an ENVI-met simulation of the thermal environment of Yanzhong Square Park in Shanghai. *Urban For. Urban Green.* **2021**, *66*, 127384. [\[CrossRef\]](#)
63. Zhang, S.J.; Li, S.Z.; Shu, L.; Xiao, T.Q.; Shui, T.T. Landscape Configuration Effects on Outdoor Thermal Comfort across Campus-A Case Study. *Atmosphere* **2023**, *14*, 270. [\[CrossRef\]](#)
64. Robitu, M.; Musy, M.; Inard, C.; Groleau, D. Modeling the influence of vegetation and water pond on urban microclimate. *Sol. Energy* **2006**, *80*, 435–447. [\[CrossRef\]](#)
65. Schaefer, M.; Ebrahimi Salari, H.; Kockler, H.; Thinh, N.X. Assessing local heat stress and air quality with the use of remote sensing and pedestrian perception in urban microclimate simulations. *Sci. Total Environ.* **2021**, *794*, 148709. [\[CrossRef\]](#)

**Disclaimer/Publisher's Note:** The statements, opinions and data contained in all publications are solely those of the individual author(s) and contributor(s) and not of MDPI and/or the editor(s). MDPI and/or the editor(s) disclaim responsibility for any injury to people or property resulting from any ideas, methods, instructions or products referred to in the content.